Table 4. Hot water energy use per person (kWh/per day) in the four buildings of SV–3

	Building UAA	Building UDC	Building UEB	Building UFA	All buildings
Weekdays	0.76	0.83	0.73	1.00	0.91
Weekends	0.96	1.16	1.14	1.26	1.13
Mean annual	0.82	0.92	0.85	1.07	0.83

Greek families. This is the reason that these patterns do not coincide with those proposed by researchers of other countries, like Perlman and Mills (1985) in Canada or Merrigan (1988) in the U.S.A.

Figures 2(a) and 2(b) show the average hourly hot water use pattern over weekdays and weekends, respectively. The weekday peak appears at 22:00, and the weekends peak at 18:00. The weekend pattern is most uniformly distributed.

Figure 3 illustrates the effect of family size on the average hot water consumption. The results of the study showed that the average hot water use per person and day reaches a peak at a family size of two or three persons and declines slightly for larger families. When the maximum hot water use per person is considered, families with four members consume more than the others.

Further analysis indicated that the members of most families consume between 25 and 35 lt/per day (see Fig. 4) and the overall average hot water consumption per person is 32.2 lt/day. This value agrees with the results of Pafelias (1988) after measurements in 13 thermosiphon systems in Greece. The majority of the families, approximately 74%, consume less than 40 lt/per day and 64% of the families consume less than 35 lt/per day.

Figures 5(a) and 5(b) show the average hourly hot water energy use pattern over weekdays and weekends, respectively. These patterns differ only slightly from the hot water use patterns and have the same characteristics. The energy consumption per person and day is given in Table 4. The maximum consumption appears during weekends and the average daily consumption by day of the week is given in Fig. 6. It is important to note that the mean annual daily consumption is only 0.83 kWh per person.

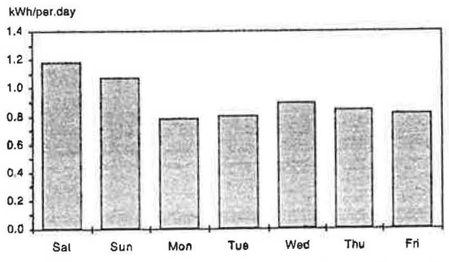

Fig. 6. Average daily hot water energy use per person—by day (all families).

There is scope for further research in this area, using the present results as a base. The analysis of the data from the monitoring of the other building of SV–3, as well as from the monitoring of individual appartments, could extend the present level of knowledge in this topic. Further analysis could also be done on the effect of various influencing factors, such as season of the year, composition of the families, age of the persons, presence of the members of the family in house, and use of various appliances that consume hot water. Using the same data, a parallel study could be done on the energy use patterns associated with hot water use in each season of the year. The knowledge of the hot water use pattern and the daily energy use are important in the design of central hot water systems.

Acknowledgments—This work was supported by the Solar Village 3 Co., under Contract 2277/28.11.88. It forms part of a research project signed in 1981 between the Greek and the German governments for the construction of a prototype urban settlement, on behalf of the Greek Organisation of Workers Dwellings (OEK).

REFERENCES

D. A. Bozis and B. A. Sotiropoulos, SV–3 measuring and evaluation phase—Final report, Region F—Building UFA, Report R/SV/FIN 4/02.92, Aristotle Univ. of Thessaloniki, PED Lab., Thessaloniki (1992).

A. C. Christoforidis, N. E. Papageorgiou, and B. A. Sotiropoulos, SV–3 measuring and evaluation phase—Final report, Region E—Building UEB, Report R/SV/FIN 3.2/02.92, Aristotle Univ. of Thessaloniki, PED Lab., Thessaloniki (1992).

T. J. Merrigan, Residential hot water use in Florida and North Carolina, *ASHRAE Trans.*, **94**, Part 1, p. 1099 (1988).

T. A. Pafelias, Hot water and energy use in residential solar DHW systems in Greece, *Proceedings 3rd National Conference on Renewable Energy Sources*, Institute of Solar Technology, Thessaloniki, Greece, Vol 1, p. HEE 39 (1988).

K. G. Paspalas, K. T. Papakostas, and B. A. Sotiropoulos, SV–3 measuring and evaluation phase—Final report, Region D—Building UDC, Report R/SV/FIN 2.3/02.92, Aristotle Univ. of Thessaloniki, PED Lab., Thessaloniki (1992).

M. Perlman and B. Mills, Development of residential hot water use patterns, *ASHRAE Trans.* **91**, Part 2, 657 (1985).

D. E. Prapas, N. Papadopoulos, and B. A. Sotiropoulos, SV–3 measuring and evaluation phase—Final report, Region A—DHW systems UAA and UAB, Report R/SV/FIN 1.1/02.92, Aristotle Univ. of Thessaloniki, PED Lab., Thessaloniki (1992).

Pergamon

Solar Energy, Vol. 54, No. 6, pp. 375–380, 1995

0038-092X/95 $9.50 + .00

0038-092X(95)00016-X

ON THE PERFORMANCE OF BUILDINGS COUPLED WITH EARTH TO AIR HEAT EXCHANGERS

M. Santamouris, G. Mihalakakou, A. Argiriou, and D. N. Asimakopoulos
Laboratory of Meteorology, Department of Applied Physics, University of Athens, Ippokratous 33, 106 80, Athens, Greece

Abstract—The use of earth to air heat exchangers has gained an increasing acceptance during the recent years. However, there is a lack of calculation models coupling the performance of the exchangers with the building. The present paper deals with the development of a new integrated method to calculate the contribution of the earth to air heat exchangers to reduce the cooling load of the buildings. The method is based on the principle of balance point temperature and permits the calculation of the hourly value of the balance temperature of the building as well as the daily cooling load of the building and the contribution of the buried pipes. An extensive validation procedure has been followed using data from an extended version of TRNSYS including detailed routines to simulate dynamically the performance of earth to air heat exchangers. It is found that the method is of sufficient accuracy and, therefore, can be used during the predesign and design phase for the dimensioning of the buried pipes.

1. INTRODUCTION

The use of the ground for heating and cooling of buildings has gained an increasing acceptance during the last years. Earth to air heat exchangers consist of pipes buried in the ground where air is forced in order to be heated or cooled and then is circulated inside the building. Recent applications and studies have shown that the use of earth to air heat exchangers, appropriately coupled with buildings, can provide an important part of their heating and cooling load, (Tombazis *et al.*, 1990; Triantis *et al.*, 1993; G. Agas *et al.*, 1991).

The use of such a system requires a difficult dimensioning process which involves optimisation of various parameters such as the airflow, length, depth, and diameter. Various algorithms to calculate the performance of a single or multiple earth to air heat exchanger have been proposed (Mihalakakou *et al.*, 1994a; G. Schiller, 1982; Santamouris and Lefas, 1986; Levit *et al.*, 1989; Chen *et al.*, 1983). A comparative analysis of the accuracy of the eight different algorithms predicting the performance of earth to air heat exchangers is given by Tzaferis *et al* (1992).

Calculation of the thermal performance of buildings using such a system requires coupling of exact building simulation codes such as TRNSYS, ESP, DOE, etc. with appropriate routines simulating the performance of the exchangers. Although there have been important research efforts on this topic (Mihalakakou, 1994; Clarke, 1994), the existing simulation tools have not yet included such a kind of routine, or the developed prototypes are not commercially available. Also, possible use of such combinations is appropriate during the detailed design phase and requires important calculation effort. Therefore, there is a need for the development of accurate, integrated codes to calculate the contribution of the earth to air heat exchangers to the building's cooling load.

The present paper deals with the development of such an integrated code. The presented algorithms are based on the well known principle of "Balance Point Temperature," (Kusuda, 1976) and are validated against extensive and detailed simulations and experimental data. The method can be used easily to calculate the contribution of the earth to air heat exchangers to the reduction of the cooling load of the buildings. The method is more reliable for the predesign phase of the building, and can be very useful during the decision process. For the final stages of the design, exact simulation tools can be used if necessary (Mihalakakou *et al.*, 1994a).

2. DESCRIPTION OF THE ALGORITHMS

The instantaneous cooling load, Q_c, for an A/C building can be written as following

$$Q_c = [k(T_o - T_i) + Q_s + Q_{in}]^+ \qquad (1)$$

where k is the building load coefficient, (W/C), T_o is the ambient temperature (C), T_i is the indoor temperature (C), Q_s is the critical part of the solar "gains" entering to the building through transparent and opaque elements in (W), and Q_{in} is the critical percentage of the internal gains (W).

Critical is defined as that part of the solar or internal load that contributes to the cooling load of the building. It is mainly the function of the building's thermal capacitance, operating schedule, shading, type of glazing, etc. Some methods to calculate the critical, or "useful," level of the solar and internal load have been proposed by Bida and Kreider (1987), ASHRAE (1991) and Baker (1987). If $Q_T = Q_s + Q_{in}$, then:

$$Q_c = [k(T_o - T_i) + Q_T]^+. \qquad (2)$$

If a balance temperature, T_b is used where:

Table 1. Characteristics of buildings simulated to calculate the cooling load

Number	Floor Surface (m^2)	Characteristics	Set Point Temperature (C)
1	100	Noninsulated, 8 cm of concrete, 3 ach	26
2	100	As above	27
3	100	As above	28
4	100	As above	29
5	100	Well insulated, 4 cm of concrete + 10 cm of insulation + 4 cm of concrete, 1 ach	26
6	100	As above	27
7	100	As above	28
8	100	As above	29
9	2500	Well insulated, 4 cm of concrete + 10 cm of insulation + 4 cm of concrete, 1 ach	26
10	2500	As above	27
11	2500	As above	28
12	2500	As above	29
13	10000	Well insulated, 4 cm of concrete + 10 cm of insulation + 4 cm of concrete, 1 ach	26
14	10000	As above	27
15	10000	As above	28
16	10000	As above	29
17	400	Well insulated, 4 cm of concrete + 10 cm of insulation + 6 cm of concrete, 1 ach	26
18	400	As above	27
19	400	As above	28
20	400	As above	29
21	400	Walls: Precast sandwich consisting of 75 mm dense concrete, 25 mm expanded polystyrene and 150 mm lightweight concrete. Roof: 15 mm Asphalt, on lightweight concrete screed, 75 mm on dense concrete 150 mm. 1 ach day and night.	26
22	400	As above	27
23	400	As above	28
24	400	As above	29
25	900	As above	26
26	900	As above	27
27	900	As above	28
28	900	As above	29
29	900	As above but 0.1 ach during night	26
30	900	As above	27
31	900	As above	28
32	900	As above	29
33	10000	Opaque Elements: 4 cm dense concrete, 10 cm polystyrene, 4 cm dense concrete. 20 sq. m of south window.	26
34	900	As above	27
35	900	As above	28
36	900	As above	29
37	900	Opaque Elements: 4 cm dense concrete, 10 cm polystyrene, 4 cm dense concrete. 10 sq. m of south window.	26
38	900	As above	27
39	900	As above	28
40	900	As above	29

$$T_b = T_i - Q_T/k, \tag{3}$$

the instantaneous cooling load can be calculated as a linear function of the outdoor temperature T_o.

$$Q_c = [k(T_o - T_b)]^+ \tag{4}$$

The daily or monthly cooling load, Q_{cm}, can be calculated by integration of eqn (4) over a day or a month. Therefore:

$$Q_{cm} = 3600\ k\ \mathrm{CDH}(T_b) \tag{5}$$

where $\mathrm{CDH}(T_b)$ are the cooling degree hours based on the hourly value of the balance temperature, T_b, for a day or a month, respectively.

Based on the above well-known theory, the instantaneous cooling load, Q_{cb}, of a building equipped with earth to air heat exchangers can be written as following:

$$Q_{cb} = [k(T_o - T_i) + Q_T - Q_{BP}]^+ \tag{6}$$

where Q_{BP} is the rate of energy offered from the buried pipes. Also, it is defined:

$$T_{pb} = T_i - (Q_T - Q_{BP})/k \tag{7}$$

where T_{pb} is the balance temperature for buildings equipped with buried pipes. Therefore, the cooling load is given by the following expression:

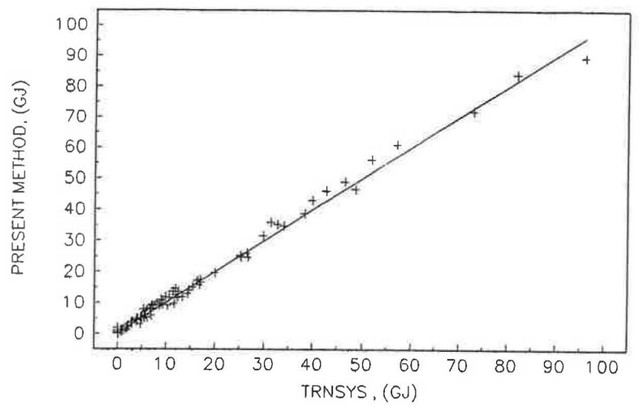

Fig. 1. Comparison of the predicted cooling load of buildings without the use of earth to air heat exchangers using TRNSYS and the present method.

$$Q_{cb} = [k(T_o - T_{pb})]^+. \tag{8}$$

The daily or monthly cooling load, Q_{cbp}, can be calculated by integration of eqn (8). Therefore,

$$Q_{cbp} = 3600\ k\ \mathrm{CDH}(T_{pb}) \tag{9}$$

where $\mathrm{CDH}(T_{pb})$ are the daily or monthly modified cooling degree hours for buildings equipped with buried pipes calculated by the following expression:

$$\mathrm{CDH}(T_{pb}) = \Sigma\ (T_o - T_{pb})S_j$$
$$S_j = 1 \text{ if } T_o > T_{pb}$$
$$S_j = 0 \text{ if } T_o \le T_{pb}. \tag{10}$$

For the calculation of the rate of energy offered by the buried pipes, Q_{BP}, the following expression is used:

$$Q_{BP} = mc\ \mathrm{DDBP}/t \tag{11}$$

where m and c are the mass flow rate and the specific heat of the circulated air, respectively. Also, t is the operational period of the exchangers, and DDBP are the degree hours for buried pipes defined as following:

$$\mathrm{DDBP} = \Sigma\ (T_o - T_{bpx})S_j$$
$$S_j = 1 \text{ if } T_o > T_{bpx} \text{ and } T_i > T_{bpx}$$
$$S_j = 0 \text{ if } T_o \le T_{bpx}$$
$$S_j = 0 \text{ if } T_o > T_{bpx} \text{ and } T_i < T_{bpx} \tag{12}$$

where T_{bpx} is the exit temperature of the air from the pipes. The buried pipes degree hours are calculated for the entire daytime period. For climates with warm nights, DDBP can be calculated for the whole day with a nonzero cooling load during that period increasing, therefore, the time, t, of eqn (11).

Therefore, the percentage of the contribution of the earth to air heat exchangers to the cooling load of the building is equal to:

$$f = [Q_{cm} - Q_{cbp}]/Q_{cm}. \tag{13}$$

To calculate the exit air temperature from the buried pipes, T_{bpx}, simplified or detailed simulation methods can be used (Mihalakalou *et al.*, 1994a; Schiller, 1982; Santamouris and Lefas, 1986; Levit *et al.*, 1989; Chen *et al.*, 1983). An accurate and easy way to apply the parametric prediction model is proposed by Mihalakakou *et al* (1994a). According to this model a dimensionless coefficient, U, is defined:

$$U = [T_{bpx} - T_{und}]/[T_{in} - T_{und}] \tag{14}$$

where T_{bpx}, T_{in}, and T_{und} are the air temperature at the pipe's outlet, the air temperature at the pipe's inlet, and the undisturbed soil temperature, respectively. The U value, and respectively T_{bpx}, is calculated by the following expression:

$$U = U_{ref}(L)\mathrm{CF} \tag{15}$$

where $U_{ref}(L)$ is a reference value of U calculated for standard values of air flow rate and depth and CF is a correction factor. The value of U_{ref} for a specific length, L, is calculated from the following expression:

$$U_{ref}(L) = a_o + a_1(L) + a_2(L)^2 + a_3(L)^3 \tag{16}$$

where a_i is the coefficient given by Mihalakakou *et al.* (1994c). Also, the correction coefficient CF is the calculated by the expression:

$$\mathrm{CF} = [b_o + b_1(D) + b_2(D)^2 + b_3(D)^3] \times [c_o + c_1(SV) + c_2(SV)^2 + c_3(SV)^3] \tag{17}$$

where D is the depth of the buried pipe below the earth surface and SV is the air volume through the exchanger. The values of b_i and c_i for various L, SV, and D are given by Mihalakakou *et al.* (1994c). The method is validated against an extensive set of experimental data and is found to be sufficiently accurate.

Table 2. Characteristics of buildings simulated to calculate the cooling load when earth to air heat exchangers are used

Number	Floor Surface (m^2)	Characteristics	Set Point Temperature (C)
1–4	100	Noninsulated, 8 cm of concrete, 1 ach, 2 heat exchangers. Depth: 1.5 m. Air Speed: 8 m/sec. Length: 20 m. Diameter: 20 cm.	26, 27, 28, 29
5–8	100	Roof + walls: 4 cm of concrete + 10 cm of insulation + 4 cm of concrete, 1 ach. 2 heat exchangers. Depth: 1.5 m. Air speed: 8 m/sec. Length: 20 m. Diameter: 20 cm.	26, 27, 28, 29
9–12	2500	Well-insulated, 4 cm of concrete + 10 cm of insulation + 4 cm of concrete, 1 ach. 3 heat exchangers. Depth: 1.5 m. Air speed: 8 m/sec. Length: 20 m. Diameter: 20 cm.	26, 27, 28, 29
13–16	10000	Well insulated, 4 cm of concrete + 10 cm of insulation + 4 cm of concrete, 1 ach. 3 heat exchangers. Depth: 1.5 m. Length: 20 m. Diameter: 20 cm.	26, 27, 28, 29
17–20	400	Walls: Precast sandwich consisting of 75 mm dense concrete, 25 mm expanded polystyrene and 150 mm lightweight concrete. Roof: Asphalt 15 mm on lightweight concrete screed 75 mm on dense concrete 150 mm. Day: 1 ach, Night: 5 ach. Use of three earth to air heat exchangers. Depth: 1.5 m. Air speed: 8 m/sec. Length: 20 m. Diameter: 20 cm	26, 27, 28, 29
21–32	900	Opaque Elements: 4 cm dense concrete, 10 cm polystyrene, 4 cm dense concrete. 10 sq. m of south window. Use of two, three, and five heat exchanger, Depth: 3 m. Length: 30 m. Diameter: 25 cm. Air velocity: 8 m/sec.	26, 27, 28, 29
33–44	900	Same building. Use of two, three, and five exchangers. Depth: 3 m. Length: 20 m. Diameter: 25 cm. Air velocity: 8 m/sec.	26, 27, 28, 29
45–56	900	Same building. Use of two, three, and five exchangers. Depth: 3 m. Length: 30 m. Diameter: 25 cm. Air velocity: 8 m/sec.	26, 27, 28, 29
57–68	900	Same building. Use of two, three, and five exchangers. Depth: 3 m. Length: 30 m. Diameter: 25 cm. Air velocity: 8 m/sec.	26, 27, 28, 29
69–80	900	Same building. Use of two, three, and five exchangers. Depth: 3 m. Length: 40 m. Diameter: 25 cm. Air velocity: 8 m/sec.	26, 27, 28, 29
81–92	900	Same building. Use of two, three, and five exchangers. Depth: 3 m. Length: 45 m. Diameter: 25 cm. Air velocity: 8 m/sec.	26, 27, 28, 29
93–104	900	Same building. Use of two, three, and five exchangers. Depth: 3 m. Length: 50 m. Diameter: 25 cm. Air velocity: 8 m/sec.	26, 27, 28, 29
105–117	900	Same building. Use of two, three, and five exchangers. Depth: 3 m. Length: 60 m. Diameter: 25 cm. Air velocity: 8 m/sec.	26, 27, 28, 29
118–129	900	Same building. Use of two, three, and five exchangers. Depth: 3 m. Length: 60 m. Diameter: 25 cm. Air velocity: 8 m/sec.	26, 27, 28, 29
130–141	900	Same building. Use of two, three, and five exchangers. Depth: 3 m. Length: 30 m. Diameter: 20 cm. Air velocity: 8 m/sec.	26, 27, 28, 29
142–153	900	Same building. Use of two, three, and five exchangers. Depth: 3 m. Length: 30 m. Diameter: 30 cm. Air velocity: 8 m/sec.	26, 27, 28, 29
154–165	900	Same building. Use of two, three, and five exchangers. Depth: 3 m. Length: 30 m. Diameter: 36 cm. Air velocity: 8 m/sec.	26, 27, 28, 29
166–182	900	Same building. Use of two, three, and five exchangers. Depth: 3 m. Length: 30 m. Diameter: 40 cm. Air velocity: 8 m/sec.	26, 27, 28, 29
183–194	900	Same building. Use of two, three, and five exchangers. Depth: 3 m. Length: 30 m. Diameter: 25 cm. Air velocity: 5 m/sec.	26, 27, 28, 29
195–206	900	Same building. Use of two, three, and five exchangers. Depth: 3 m. Length: 30 m. Diameter: 25 cm. Air velocity: 9 m/sec.	26, 27, 28, 29
207–218	900	Same building. Use of two, three, and five exchangers. Depth: 3 m. Length: 30 m. Diameter: 25 cm. Air velocity: 7 m/sec.	26, 27, 28, 29
219–230	900	Same building. Use of two, three, and five exchangers. Depth: 3 m. Length: 30 m. Diameter: 25 cm. Air velocity: 10 m/sec.	26, 27, 28, 29
231–242	900	Same building. Use of two, three, and five exchangers. Depth: 2 m. Length: 30 m. Diameter: 25 cm. Air velocity: 8 m/sec.	26, 27, 28, 29
243–254	900	Same building. Use of two, three, and five exchangers. Depth: 4 m. Length: 30 m. Diameter: 25 cm. Air velocity: 8 m/sec.	26, 27, 28, 29
255–266	900	Same building. Use of two, three, and five exchangers. Depth: 4.5 m. Length: 30 m. Diameter: 25 cm. Air velocity: 8 m/sec.	26, 27, 28, 29
267–278	900	Same building. Use of two, three, and five exchangers. Depth: 5 m. Length: 30 m. Diameter: 25 cm. Air velocity: 8 m/sec.	26, 27, 28, 29
279–290	900	Same building. Use of two, three, and five exchangers. Depth: 5.5 m. Length: 30 m. Diameter: 25 cm. Air velocity: 8 m/sec.	26, 27, 28, 29
291–302	900	Same building. Use of two, three, and five exchangers. Depth: 6 m. Length: 30 m. Diameter: 25 cm. Air velocity: 8 m/sec.	26, 27, 28, 29

3. VALIDATION PROCEDURE AND RESULTS

In order to verify the accuracy of the previously proposed algorithms to calculate the cooling load of A/C buildings coupled with earth to air heat exchangers, comparisons of the calculated monthly cooling load have been performed for various types of buildings and configurations. Calculations have been performed using the previously described algorithms and an extensive version of the TRNSYS simulation programme (TRNSYS, 1990) coupled with algorithms to simulate dynamically the performance of the earth to air heat exchangers.

As a first step, and in order to validate the accuracy of the algorithms to calculate the cooling load of buildings before coupling with the earth to air heat exchangers, the cooling load of buildings has been calculated using the algorithms presented in eqns (1–5) and then TRNSYS. The main characteristics of the simulated buildings are given in Table 1. The method proposed by Baker (1987) to calculate the useful solar and internal gains in a daily basis is used. All simulations have been carried out considering that buildings are continuously thermostatically controlled. For the majority of the studied buildings, indoor temperatures during the night were lower than the set point temperature and, thus, buildings were free-floating during the night. However, as the method is based on hourly calculations, the fact that buildings may operate as free-floating during a time period is already taken into account in the calculation of the cooling degree hours and, thus, the accuracy of the method is not affected.

The results of the monthly as well as of the annual cooling load as calculated by TRNSYS and the present method are given in Fig. 1. As shown there is a very good agreement between the two sets of data. Regarding the annual cooling load, the absolute difference between the two sets of values is between 0.0 and 15% with a mean value close to 6.3%. The absolute difference between the monthly predicted values is between 0.0 and 25%.

At a second step, and in order to validate the accuracy of the algorithms proposed to calculate the performance of buildings coupled with earth to air heat exchangers in eqns (6–12), comparisons have been performed with a version of TRNSYS coupled with a transient numerical model describing the performance of earth to air heat exchangers (Mihalakakou *et al.*, 1994a; Mihalakakou *et al.*, 1994b). The transient numerical model used to calculate the thermal performance of a single buried pipe, as well as of multiple parallel earth to air heat exchangers, has been developed and is presented by Mihalakakou (1994b).

This model takes into account the coupled and simultaneous movement of heat and moisture in the soil under a temperature gradient, as well as the vertical thermal stratification in the soil, which breaks down the axial symmetry of heat flow from the pipe. It includes a complete mathematical description of moisture migration through the soil under a thermal gradient from higher to lower temperature regions, while it simultaneously redistributes itself in reverse order due to the resulting moisture gradient. The natural thermal stratification is taken into account with ground surface boundary conditions. The thermal model was entirely developed inside the TRNSYS environment.

The model was validated against an extensive set of experimental data and was found to accurately predict the temperature and the humidity of the circulating air, the distribution of the temperature and moisture into the soil, as well as the overall thermal performance of the earth to air heat exchangers.

Three hundred and two various scenarios involving different building characteristics, number of pipes, indoor temperature, depth, diameter, air velocity, and pipe length have been performed. The studied cases are summarised in Table 2. Climatic data of Athens, Greece, have been used.

The results of the monthly and annual cooling loads as obtained from the dynamic simulation as well as from the present method are plotted in Fig. 2. As shown, there is a very good agreement between the two sets of data. Regarding the estimated annual cooling loads, the obtained differences are between 1.0 and 8%. The higher values are presented for the low cooling loads. As it concerns the monthly cooling load predictions, the differences are between 0.0 and 15%. Therefore, the proposed method is of sufficient accuracy and can be used

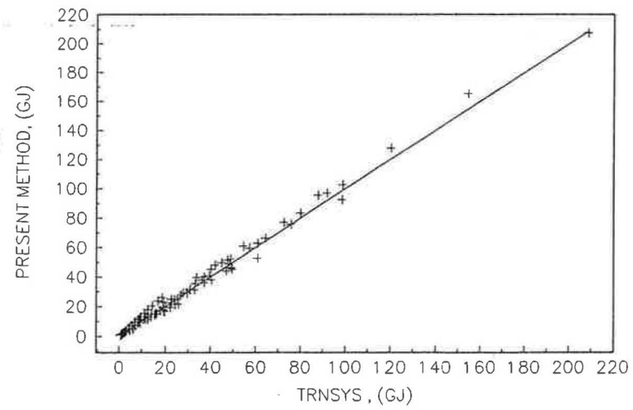

Fig. 2. Comparison of the predicted cooling load of buildings using earth to air heat exchangers using TRNSYS and the present method.

to predict the contribution of the earth to air heat exchangers to the cooling load of a building.

4. CONCLUSION

A new integrated method to calculate the contribution of the earth to air heat exchangers to the cooling load of the buildings is presented. The method is based on the principle of balance point temperature and permits the calculation of the hourly value of the balance temperature of the building as well as the daily cooling load and the contribution of the buried pipes. An extensive validation procedure has been followed using data from an extended version of TRNSYS which includes detailed routines to simulate dynamically the performance of earth to air heat exchangers. It is found that the method is of sufficient accuracy and, therefore, can be used during the predesign and design phase for the dimensioning of the buried pipes.

REFERENCES

G. Agas, T. Matsagos, M. Santamouris, and A. Argiriou, On the use of the atmospheric heat sinks for heat dissipation, *Energy and Buildings* **17,** 321–329 (1991).

ASHRAE, *Handbook of fundamentals,* ASHRAE, Atlanta, GA (1991).

N. Baker, *Passive and low energy building design for tropical island climates,* Prepared for the Commonwealth Science Council by the ECD Partnership, London (1987).

M. Bida and J. F. Kreider, Monthly averaged cooling load calculations—Residential and small commercial buildings, *J. Solar Energy Engineering* **109,** 311–320 (1987).

B. Chen, T. Wang, J. Maloney, and M. Newman, Measured and predicted cooling performance of earth contact tubes *Proc. 1983 Annual Meeting of ASES,* ASES, MN (1983).

J. Clarke, *Private information on the coupling of ESP with earth to air heat exchangers,* University of Strathclyde, Glasgow, UK (1994).

T. Kusuda, *National Bureau of Standards Heating and Cooling Load Determination Program,* NBS BSS 69 (July, 1976).

H. Levit, R. Gaspar, and R. D. Piacentini, Simulation of greenhouse micro climate by earth tube heat exchangers, *Agric. Forest Meteorol.,* 31–47 (1989).

G. Mihalakakou, *On the use of the ground for heat dissipation,* Ph.D. Project Report on the coupling of earth to air heat exchangers with TRNSYS, University of Athens, Department Applied Physics, Athens (1994).

G. Mihalakakou, M. Santamouris, and D. N. Asimakopoulos, Modelling the thermal performance of the earth to air heat exchangers, *Solar Energy* **53**(3), 301–307 (1994a).

G. Mihalakakou, M. Santamouris, and D. Asimakopoulos, Use of the ground for heat dissipation, *Energy* **19**(1), 17–25 (1994b).

G. Mihalakakou, M. Santamouris, D. Asimakopoulos, and I. Tselepidaki, Parametric prediction of the buried pipes cooling potential for passive cooling applications, *Solar Energy* (in press).

M. Santamouris, and C. C. Lefas, Thermal analysis and computer control of hybrid greenhouses with subsurface heat storage, *J. Energy in Agriculture* **5,** 161–173 (1986).

G. Schiller, Earth tubes for passive cooling: The development of a transient numerical model for predicting the performance of earth to air heat exchangers, Project Report for M.Sc. Degree, Massachusetts Institute of Technology, Cambridge, MA, (June, 1982).

A. Tombazis, A. Argiriou, and M. Santamouris, Performance evaluation of passive and hybrid cooling components for a hotel complex, *Int. J. Solar Energy* **9,** 1–12 (1990).

E. Triantis, M. Santamouris, A. Argiriou, and M. Valindras, Thermal performance evaluation of a passive solar atrium in Greece, *Proc. 3rd European Conference on Architecture,* pp 618–621, Sir N. Foster, H. Scheer, (Editors), Organized by the Commission of the European Communities, H. S. Stephens and Associates Publishers, Florence (17–21 May, 1993).

TRNSYS 13.1, *A transient system simulation program developed from solar energy laboratory,* University of Wisconsin-Madison, Madison, WI (1990).

A. Tzaferis, D. Liparakis, M. Santamouris, and A. Argiriou, Analysis of the accuracy and sensitivity of earth to air heat exchangers, *Energy and Buildings* **18,** 35–43 (1992).

Pergamon

Solar Energy, Vol. 54, No. 6, pp. 381–385, 1995

0038-092X/95 $9.50 + .00

0038-092X(95)00005-4

TOWARD A THEORETICAL LIMIT OF SOLAR CELL EFFICIENCY WITH LIGHT TRAPPING AND SUB-STRUCTURE

F. PELANCHON and P. MIALHE*
Centre d'Electronique de Montpellier, Université Montpellier II, 34095 Montpellier Cedex 05- France;
*Centre d'Etudes Fondamentales, Université de Perpignan, Avenue de Villeneuve, 66860 Perpignan Cedex France

Abstract—The performances of Si – n^+ – p solar cells are calculated using the cell width as a parameter and taking into account light trapping effect and infrared light excitation due to the inclusion of a defect layer near the $n-p$ junction. A model is developed to describe light confinement and optimized cell structures are considered. The low absorption of long wavelength photons in thin solar cells is shown to be compensated by the light confinement. Higher values of the maximum output power are obtained and the effect is particularly significant for thin base cells ($H < 60$ μm) with a 3.5 mW cm^{-2} maximal increase of the maximum output power.

1. INTRODUCTION

Terrestrial utilization of silicon solar cells as a possible source of electric power requires the development of low cost devices to compete economically with conventional energy sources. Modelling and simulation techniques have shown that large scale manufacturing requires new cell structures with a higher efficiency and a smaller material consumption.

The optical absorption properties of silicon dictate that crystal cells should be made of 300 μm Si layers in order to optimize electron-hole pair creation ability. Sah (1986) has pointed out that the limiting efficiency of such structures is imposed by energy losses via carrier recombination resulting from transport processes. Studies proposed by Pélanchon and Mialhe (1990a) and Pélanchon (1992) of the minority carrier distribution, according to the base width and to the base doping level, lead to the consideration of thin Si-solar cell structures. This work results in the definition of a device with higher values of the open-circuit voltage and of the maximum output power. In these thin base solar cells ($H \leq 50$ μm), the low absorption of long wavelength photons, which reduces the photocurrent by a few mAcm^{-2}, is partly compensated by the decrease of the bulk recombination with a back surface acting as a mirror for the minority carriers. The addition of confinement with defect thin structures can theoretically improve performances.

Li *et al.* (1992) have reported an increase of silicon cell efficiency by the inclusion of a local defect layer near the n–p junction, consisting of a strongly modified Si material (by ion implantation [Li *et al.,* 1992; Zammit *et al.,* 1991], structural deformation, etc.) This layer results in sub-band gap excitation processes which involve carrier creations by infrared light excitations via defect levels. In order to avoid recombination enhancement due to this substructure, which reduces the final photocurrent (Summonte *et al.,* 1992, 1993), Kuznicki *et al.* (1993a, 1993b) proposed to equip the edges of the sub-structure with two L–H (Low–High) interfaces with ∂-doping properties (around 10^{20} cm^{-3}). These interfaces create strong electric fields that drift generated electron-hole pairs away from the sub-structure. The optimal sub-structure is likely to consist of a middle-band gap defect layer which allows absorption of two infrared photons (Rohatgi *et al.,* 1993). Nevertheless, to be noteworthy, this L–H improvement needs cell structures which ensure absorption of all the photons whose energy is greater than the energy band gap. To obtain such an absorption, when using thin base solar cells, the cell structure requires an optical confinement consisting of several reflections of photon rays inside the cell. This would necessitate the manufacturing of structures that increase internal reflection without degrading carrier generation and collection (Rohatgi *et al.,* 1993; Tiedje *et al.,* 1984; Luque, 1991; Willeke *et al.,* 1992; Smith *et al.,* 1993; Wang *et al.,* 1990). Then, this light trapping yields an enhancement of the absorbance, $a(\lambda)$, for photons with energy greater than 1.12 eV.

In this paper, the influence of light trapping on solar cell performances is modeled. The photocurrent is computed and the maximum output power is determined according to the cell width for optimized cell parameters values including parameter relationships which are imposed by current technology, cell specifications, and operating conditions. An optimum base width appears for maximum light trapping effects.

2. PHOTOCURRENT

It is assumed that each photon, with energy greater than 1.12 eV (wavelength $\lambda \leq 1.08$ μm), when absorbed, creates an electron-hole pair in the cell structure (absorption by free carriers is neglected).